2A12T4 铝合金焊接时拘束条件对热裂纹的影响

李 军[1,2]， 杨建国[1]， 闫德俊[1]， 方洪渊[1]
（1. 哈尔滨工业大学 现代焊接生产技术国家重点实验室，哈尔滨 150001；
2. 广州有色金属研究院，广州 510651）

李 军

摘 要：采用一种简便有效的热裂纹试验方法，在普通刚性焊接夹具上研究了拘束力和拘束距离对 2A12T4 铝合金焊接热裂倾向的影响. 结果表明，保持拘束距离不变，随着拘束力的增加，焊接热裂纹率逐渐减小，当拘束力到达一定值后，热裂纹率趋于稳定；保持拘束力不变，随着拘束距离增加，焊接热裂纹率呈增加趋势. 夹具对工件的拘束条件主要是通过影响焊件的回转变形程度和焊缝区金属的冷却收缩速度来影响焊接热裂倾向.

关键词：铝合金；焊接；拘束条件；热裂纹
中图分类号：TG407 文献标识码：A 文章编号：0253－360X(2009)07－0069－04

0 序 言

铝合金材料由于具有重量轻、比强度高、耐腐蚀和易成形等优良特性被广泛应用于飞机、火箭等航空航天器上. 新型的汽车、动车等民用产品为节省能源和提高性能，也越来越多地采用高强铝合金作为钢的替代品. 但铝合金一般都具有较宽的脆性温度区间，线膨胀系数较大，凝固时收缩率高，焊接时容易产生热裂纹[1,2]，从而给焊接结构的使用安全带来隐患. 为了解决铝合金的焊接热裂纹问题，国内外焊接工作者做了大量的研究工作，但这些研究往往忽略了拘束条件，使拘束状态过于苛刻或宽松，无法反映真实生产条件下热裂行为. 另外，目前关于铝合金焊接时拘束条件对焊接热裂倾向影响的研究较少，无论是科研还是实际生产都缺乏可靠的试验数据支持. 鉴于此，文中在普通刚性焊接夹具上进行了拘束力和拘束距离对 2A12T4 铝合金焊接热裂倾向影响的研究，旨在弄清拘束条件对焊接热裂倾向的影响规律，为实际生产中如何选择合理的拘束条件提供借鉴.

1 焊接热裂纹的产生机制

关于焊接热裂纹的形成，目前被普遍接受的观点是普洛霍洛夫理论，该理论认为，当焊缝金属凝固时，成分较纯的金属熔点较高，首先凝固形成枝晶的主干，而大部分合金元素及杂质仍保留在液体中，随着温度的进一步降低，枝晶慢慢长大，液态金属越来越少而杂质浓度越来越高，最后被排挤到晶界上，形成液态低熔共晶薄膜. 液态薄膜和固体金属共存的温度范围就称为脆性温度区间 BTR（图 1[3]）. 脆性温度区间的上限是枝晶开始交织长合的温度，用 T_U 表示，下限是液膜完全消失的实际固相线（略低于固相线 T_S）. BTR 区间金属的延性很小，如果受到拉应力的作用，液态薄膜就容易被拉开成为微裂纹，如果没有足够量的液态金属补充，当焊缝完全凝固以后，此裂纹就会保留下来，最终形成热裂纹.

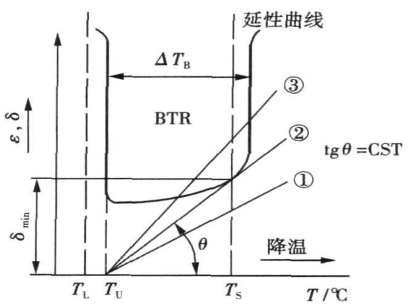

图 1 普洛霍洛夫焊接热裂纹理论
Fig. 1 Schematic of hot cracking by Prokhorov

焊接热裂纹产生的必要条件是焊缝金属在脆性

收稿日期：2008－05－07

温度区间内存在拉伸应变. 焊缝凝固过程中热裂纹的产生与三个因素有关[4−6]: 脆性温度区间的大小 ΔT_B; 焊缝金属在脆性温度区间的延性大小 δ_{min}; 焊缝金属在脆性温度区间内的拉伸应变 ε 或拉伸应变速率 $d\varepsilon/dT$. 其中脆性温度区间的大小和焊缝金属在脆性温度区间的延性主要决定于冶金因素, 而焊缝金属在脆性温度区间内的拉伸应变或拉伸应变速率主要决定于力学因素, 如焊接工艺参数和焊件的装夹状态等. 由于焊接热裂纹的产生是一个动态过程, 焊缝金属在脆性温度区间内的拉伸应变 ε 或拉伸应变速率 $d\varepsilon/dT$ 是影响焊接热裂纹产生与发展的主要因素. 当 $d\varepsilon/dT$ 小于临界应变速率 CST 时(图 1 中的①曲线), $\varepsilon < \delta_{min}$, 不会产生热裂纹; 当 $d\varepsilon/dT$ 等于临界应变速率(CST)时, (图 1 中的②曲线, $\varepsilon \approx \delta_{min}$, 为裂纹产生的临界状态; 而当 $d\varepsilon/dT$ 大于临界应变速率 CST 时(图 1 中的③曲线), 在 T_S 附近, $\varepsilon > \delta_{min}$, 则会产生热裂纹.

2 试验方法

试验材料选用厚度为 2 mm 和 1.5 mm 的 2A12T4 铝合金板, 试件尺寸及起弧点和收弧点位置如图 2 所示.

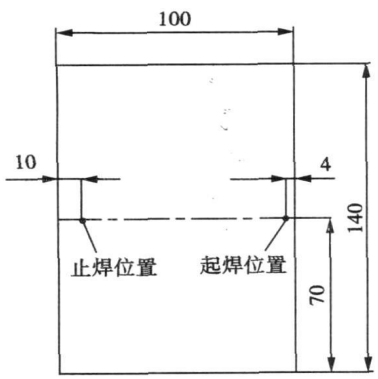

图 2 试件尺寸及起弧点和收弧点位置(mm)

Fig. 2 Dimension of test pieces and positions of arc-starting and arc-blowout

试验时作用在试件上的拘束条件由自行设计的刚性焊接夹具提供, 夹具的外形尺寸及试件的夹持位置如图 3 所示. 试验时试件置于底板和压板之间, 对两对螺栓施加不同拧紧力矩可以改变夹具对试件的拘束力, 调整两块压板之间的间距可以改变夹具对试件的拘束距离. 焊接方法采用交流钨极氩弧焊不填丝的表面熔敷方式, 焊接速度为 285 mm/min, 对应于 2 mm 和 1.5 mm 厚试件的焊接电流分别为 130 A 和 115 A.

以裂纹率 H_c(%)作为热裂倾向的评定指标, 表示为

$$H_c(\%) = \frac{L_{hc}}{L_T}$$

式中: L_{hc} 为热裂纹长度; L_T 为焊道长度. 为减少试验误差, 对应于每组试验采用 5 个平行试样.

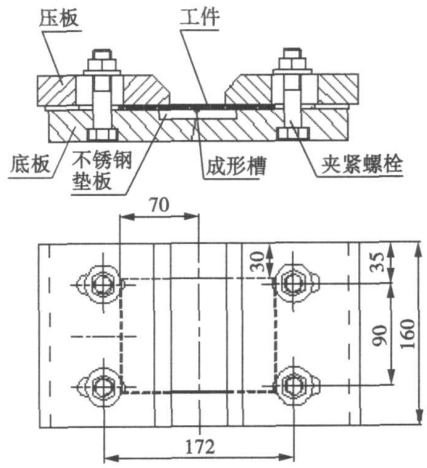

图 3 刚性焊接夹具及试件的夹持位置(mm)

Fig. 3 Schematic of rigid welding fixture and clamping position of test pieces

3 试验结果

保持图 3 中两块压板的间距为 20 mm 不变, 对两对夹紧螺栓施加不同扭矩以考察拘束力对试件热裂纹率的影响. 图 4 为拘束力对 2 mm 厚试件热裂纹率影响的统计结果. 可以看到, 当螺栓不拧紧时, 裂纹率为 79%, 随着螺栓扭矩的增加, 裂纹率逐渐减小, 当扭矩增至60 N·m时, 裂纹率减少到21%.

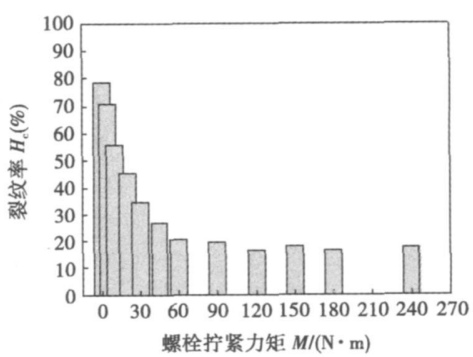

图 4 拘束力对焊接热裂纹率的影响

Fig. 4 Influence of restraint force on H_c%

但当扭矩继续增加时,裂纹率不再发生明显变化,达到一个稳定值.

图5 为拘束力对 1.5 mm 厚试件焊接热裂纹影响的实物图,该图中热裂纹长度随着拘束力增加而变化的趋势与图 4 中裂纹率的变化趋势相似,也是当拘束力较小时,裂纹长度很长,随着拘束力的增加,裂纹长度逐渐变短,当拘束力增加到一定值后,热裂纹长度不再发生大的变化.

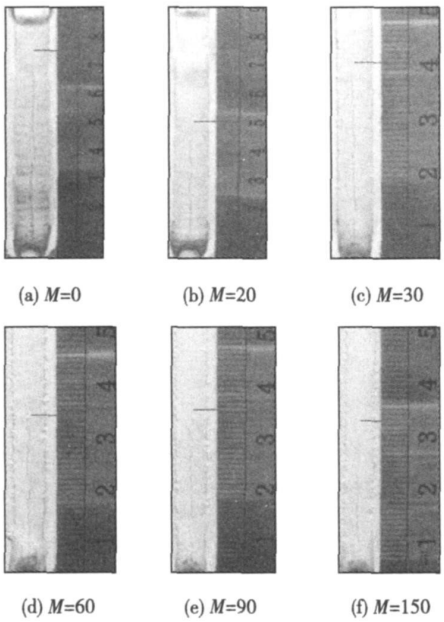

M 为螺栓扭矩,单位为 N·m

图 5　拘束力对焊接热裂纹影响的实物图

Fig. 5　Pictures of restraint force on welding hot cracking

保持夹紧螺栓的拧紧力矩为60 N·m 不变,改变两块压板的间距来考察拘束距离对试件热裂纹率的影响.图 6 为拘束距离对 2 mm 厚试件热裂纹率影响的统计结果. 可见,当拘束距离为20 mm时,裂纹率为 21%,随着拘束距离的增加,裂纹率逐渐增加,当拘束距离增至 60 mm 时,裂纹率达到了 74%.

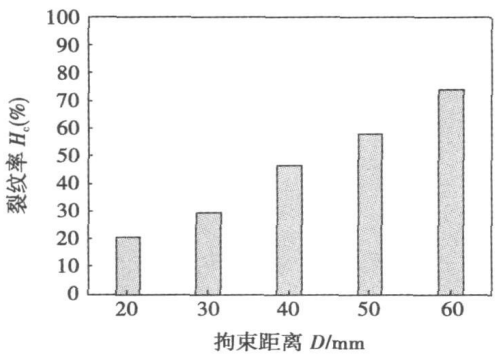

图 6　拘束距离对焊接热裂纹率的影响

Fig. 6　Influence of restraint distance on Hc%

4　分析与讨论

焊接开始后,熔池附近金属加热膨胀受到拘束会形成两个明显的压应力区[7],这两个压应力区的存在会使焊接工件产生回转变形,在回转变形的带动下,位于 BTR 区间的焊缝金属将产生拉伸应变 ε_1. 同时,由于焊缝金属在冷却过程中的凝固收缩和热收缩以及近缝区金属的热收缩,位于 BTR 区间的焊缝金属还会产生拉伸应变 ε_2. ε_1 与 ε_2 之和便构成了可能导致焊缝起弧端开裂的拉伸应变 ε,如图 7 所示.

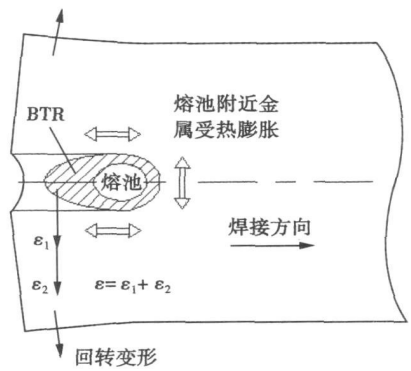

图 7　BTR 区间焊缝金属拉伸应变的产生机制示意图

Fig. 7　Schematic for generation of tensile strain of weld metal in BTR

焊接过程中工件置于底板和压板之间,通过拧紧夹紧螺栓使夹具与工件保持紧密接触. 当焊件因回转变形而朝向外侧偏转时,夹具的压板和底板就会通过对工件施加与其运动方向相反的摩擦力来阻碍焊件的回转变形. 当螺栓拧紧力矩较小时,夹具对焊件回转变形的拘束作用很小,因而 BTR 区间焊缝金属产生的拉伸应变 ε_1 及其应变速率 $\mathrm{d}\varepsilon_1/\mathrm{d}T$ 较大,但另一方面,拘束力小时工件与夹具之间的实际接触面积小,焊后冷却速度较慢,这相当于降低了夹具的散热能力,因此,由于焊缝区金属冷却收缩而导致的拉伸应变 ε_2 及其应变速率 $\mathrm{d}\varepsilon_2/\mathrm{d}T$ 均较小. 由于此时 $\mathrm{d}\varepsilon_1/\mathrm{d}T$ 与 $\mathrm{d}\varepsilon_2/\mathrm{d}T$ 之和远大于临界应变速率 CST,故热裂倾向较大. 随着螺栓拧紧力矩的增加,焊接时阻碍焊件回转变形的摩擦力相应增加,其导致 BTR 区间焊缝金属产生的拉伸应变 ε_1 和拉伸应变速率 $\mathrm{d}\varepsilon_1/\mathrm{d}T$ 都呈减小趋势,但工件与夹具的

紧密接触又会增加夹具的散热能力，使 ε_2 和 $d\varepsilon_2/dT$ 增大. 由此可见，夹具对工件拘束力的改变从两个相反方面来影响焊接热裂倾向. 分析认为，在一定的拘束力范围内，由焊件回转变形引起的拉伸应变 ε_1 的变化起主导作用，即随着拘束力的增加，ε_1 和 $d\varepsilon_1/dT$ 的减小量远大于 ε_2 和 $d\varepsilon_2/dT$ 的增加量，因此焊接热裂纹率将随拘束力的增加呈现减小趋势. 但当拘束力增大到一定值后，由于施力方式的限制，随着拘束力的增加，$d\varepsilon_1/dT$ 的减小量将趋于平缓，而工件与夹具之间紧密程度变化所引起的 $d\varepsilon_2/dT$ 的改变也呈缓慢增加的趋势，因此焊接热裂纹率基本上趋于稳定.

拘束距离对焊接热裂倾向的影响同样也可以从拉伸应变 ε_1 和 ε_2 的变化来解释. 当夹具压板拘束距离较小时，夹具对熔池后方高温金属的散热能力较强，因此 ε_2 和 $d\varepsilon_2/dT$ 较大，但此时夹具对焊件回转变形的拘束作用也比较大，因此 ε_1 及其应变速率 $d\varepsilon_1/dT$ 较小. 随着拘束距离的增加，夹具对工件的散热能力逐渐变差，这从焊缝熔宽的变化可以看出(图 8)，故 ε_2 和 $d\varepsilon_2/dT$ 逐渐减小，但与此同时，夹具作用在工件上的摩擦力逐渐减小(压强基本不变，夹具与工件接触面积的减小将导致夹具对工件的正压力减小)，因而焊件回转变形受到的拘束作用减弱，ε_1 及其应变速率 $d\varepsilon_1/dT$ 将显著增加. 如前所述，焊件回转变形引起的拉伸应变 ε_1 的变化是影响焊接热裂倾向的更重要因素，因此，随着夹具拘束距离的增加，BTR区间焊缝金属的拉伸应变速率 $d\varepsilon/dT$ 与临界应变速率 CST 的差值越来越大，故焊接热裂纹率会逐渐增加. 需要说明的是，如果拘束距离过大，焊接加热过程中焊缝部位会发生明显的隆起变形，这将导致 BTR 区间焊缝金属的冷却速度很慢，因此焊件上的热裂纹长度将急剧缩短，甚至没有热裂纹出现，此时焊接热裂率不再符合图 6 中的变化规律.

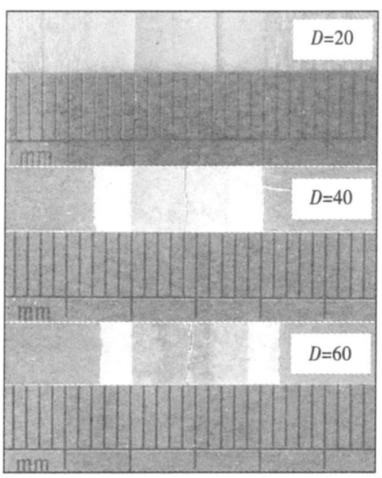

图 8 拘束距离对焊缝熔宽的影响

Fig 8 Influence of restraint distance on weld width

5 结 论

(1) 2A12T4 铝合金焊接时拘束力和拘束距离对焊接热裂倾向有显著的影响. 在一定的拘束距离范围内，拘束距离越大，热裂纹率越大；拘束力较小时，热裂纹率比较大，随着拘束力的增加，热裂纹率逐渐减小，当拘束力增大到一定值后，热裂纹率趋于稳定.

(2) 夹具拘束条件对焊接热裂倾向的影响可以从两方面解释，一是影响焊件的回转变形程度，二是影响焊缝区金属的冷却收缩速度.

(3) 焊接加热时焊件的回转变形会导致 BTR 区间焊缝金属产生拉伸应变，该拉伸应变随拘束条件的变化是影响焊接热裂倾向的主要因素.

参考文献：

[1] Shimizu S, Yamanaka E, Okuda H. Study on cracking in electron beam welding of A6061[J]. Welding International, 2001, 15(10): 776—782.

[2] Senkara J, Zhang H. Cracking in spot welding of aluminum alloy AA5754[J]. Welding Journal, 2000, 79(7): 194s—201s.

[3] Yang Y P, Dong P, Zhang J, *et al*. A hot-cracking mitigation technique for welding high-strength aluminum alloy[J]. Welding Journal, 2000, 79(1): 9s—17s.

[4] Liu W P, Tian X T, Zhang X Z. Preventing weld hot cracking by synchronous rolling during welding[J]. Welding Journal, 1996, 75(9): 297s—304s.

[5] Wilken K, Kleistner H. The classification and evaluation of hot cracking tests for weldments[J]. Welding Research Abroad, 1991, 37(11): 37—43.

[6] Herold H, Streitenberger M, Pchennikov A. Modelling of one sided welding to describe hot cracking at the end of longer butt weld seams [J]. Welding in the World, 1999, 43(2): 56—64.

[7] 李 军. 随焊旋转挤压控制铝合金薄板焊接应力变形及防热裂研究[D]. 哈尔滨：哈尔滨工业大学，2009.

作者简介：李 军，男，1973 年出生，工学博士. 主要从事焊接结构和钎料材料方面的研究工作. 发表论文 7 篇.

Email：lijun20066002@sina.com

Xuefeng (School of Materials Science and Engineering, Xi' an University of Technology, Xi' an 710048, China). p 53—56

Abstract: The rapid solidification welding of quenched Cu-Sn alloy foils with the thickness of 40—60μm was conducted by a micro-type capacitor discharge welding machine, and the effects of welding parameters on microstructural morphology and mechanical properties of joint were researched. The results indicate that welding voltage and electrode pressure have obvious influence on the shear strength of joint under fixed capacitance. With the increase of Sn content, the welding voltage needed decreases and electrode pressure rises accordingly. The favorable welding parameters are U= 90 V, F= 11 N for Cu-7%Sn alloy and U= 85 V, F= 11.5 N for Cu-13.5% Sn alloy. The main welding defect is porosity. With decreasing of welding voltage and increasing of electrode pressure, the joint cooling rate increases and the pore nucleation rate decreases. Meanwhile, the growth, mergence and migration of porosities are suppressed, resulting in the decrease of porosity forming tendency.

Key words: quenched Cu-Sn alloy; alloy foil; rapid solidification weld; shear strength

Fast transform ultra-sonic pulse TIG welding QI Bojin, XU Haiying, ZHOU Xingguo, HUANG Songtao (School of Mechanical Engineering and Automation, Beijing University of Aeronautics Astronautics, Beijing 100191, China). p 57—60

Abstract: A current fast transform ultra-sonic pulse TIG power source based on new type IGBT topology was developed. The supremest output pulse current frequency is 30 kHz. The pulse current change rate is up to 50 A per microsecond. 0Cr18Ni9Ti austenitic stainless steel was welded by this fast transform ultra-sonic pulse TIG welding and conventional DC TIG welding respectively. These joints were analyzed by X-radial check-up, tensile strength and specific elongation detection, optical-microscope and scanning electron microscope to study the difference between joints welded by different welding technologies. The result shows that fast transform ultra-sonic pulse TIG welding can refine grain and narrow the width of the coarse grain zone. These indicate that welding quality is improved by introducing fast transform ultra-sonic pulse TIG welding technology.

Key words: ultra-sonic pulse; grain refinement; welding joint

Microstructure and mechanical property of 93W/Ni/QSn4-3 joint welded by diffusion bonding SU Xiaopeng[1], LUO Guoqiang[1,2], SHEN Qiang[1], WANG Chuanbin[1], ZHANG Lianmeng[1] (1. State Key Laboratory of Advanced Technology for Materials Synthesis and Processing, Wuhan University of Technology, Wuhan 430070, China; 2. Laboratory for Shock Wave and Detonation Physics Research, Southwest Institute of Fluid Physics, CAEP, Mianyang 621900, Sichuan, China). p 61—64

Abstract: The 93W/Ni/QSn4-3 joint was prepared by diffusion bonding at vacuum using pure nickel foil as interface layer. The microstructure and composition were characterized by SEM and EPMA. The tensile strength of joint was also measured. The test results show that Ni foil improves the tensile strength of 93W/Ni/QSn4-3 joint. The thickness of Ni interlayer becomes thiner obviously because of the diffusion layer between Ni element of Ni foil and W and additional elements of 93W alloy, as well as the gradient layer of Ni and Cu elements. Solution reactions between Ni element of Ni foil and Cu element of QSn4-3 alloy, W and additional elements of 93W alloy achieve the joint of 93W/Ni/QSn4-3, that is why tensile strength of 93W/Ni/QSn4-3 joint welded is improved.

Key words: diffusion bonding; tungsten alloy; tin-bronze (QSn4-3); nickel foil

Properties and microstructures of Fe-Cr coating with high boron by plasma cladding process MA Hu, WU Yuping, WANG Guotong (School of Materials Science and Engineering, Hehai University, Nanjing 210098, China). p 65—68

Abstract: A harden coating of Fe-Cr based alloy, containing high boron, was produced on midium carbon steel plate by plasma cladding process. The phases, microstructures and microhardness of the cladding coating were investigated by Scanning Electron Microscopy (SEM), X-ray Diffractometer (XRD), Energy-dispersive Spectroscopy (EDS) and microhardness tester. The chief phases of the cladding coating are γ-Fe(Ni) and Fe_2B. The microstructures of cladding coating were consisted of Fe_2B with shapes of equilateral L or lath and eutectic of γ-Fe(Ni) and borides, and the eutectic presented itself with lamella or rosette shape. An excellent metallurgical interface between the coating and the substrate appeared. The microstructures of the layer near the interface exhibit fan-shaped or dendritic structure. The microhardness value of the cladding coating was 1 100—1 400$HV_{0.2}$ and was about 4 times of the substrate (290$HV_{0.2}$). The microhardness of the substrate near the interface increased to 600$HV_{0.2}$ because of quenching.

Key words: plasma cladding coating; microstructure; microhardness; 45 steel; heat-affected zone

Effect of restraint condition on hot cracking during welding of 2A12T4 aluminum alloy LI Jun[1,2], YANG Jianguo[1], YAN Dejun[1], FANG Hongyuan[1] (1. State Key Laboratory of Advanced Welding Production Technology, Harbin Institute of Technology, Harbin 150001, China; 2. Guangzhou Research Institute of Non-ferrous Metals, Guangzhou 510651, China). p 69—72

Abstract: A simple and effective experimental method was adopted to investigate the effects of restraint force and restraint distance on hot cracking tendency during welding of 2A12T4 aluminum alloy on the common rigid welding fixture. Experimental results show that, under the condition of keeping restraint distance unchanged, the rate of hot cracks decreases gradually with increase of restraint force and finally well reaches a stable value when the reatraint force is great enough. Keeping the restraint force unchanged, the rate of hot cracks increases with increase of restraint distance. The influence of restraint condition on tendency of hot cracking through effect-

ing the extent of externally-expanded deformation of weldment and the cooling speed of metals in and around the weld.

Key words: aluminum alloy; welding; restraint condition; hot cracking

Design of transistor-style high-frequency resistance spot-welding power supply CAO Biao, WANG Xiaodong, FAN Fengxin, LI Jianguo (College of Mechanical and Automotive Engineering, South China University of Technology, Guangzhou 510640, China). p 73—76, 80

Abstract: According to the special requirements of micro-part resistance spot welding technics, a transistor-style high-frequency power supply was designed, which could improve the control precision of the power. The main circuit structure, the working principle, and the controlling core dsPIC30F6010 were introduced. The 100 kHz frequeney was applied for the first time in the resistance spot-welding power supply field, as a result, the control accuracy and response speed were greatly increased, and the welding current waveform were excellent. It is proved that this power supply has a unique advantage in precise welding and is more adaptive, compared with other micro-part welding powers supply.

Key words: transistor-style; resistance spot-welding; dsPIC30F6010; power supply

Analysis on key technologies for pipeline internal circumferential automatic welding machine with multi-torch ZENG Huilin[1,2], DU Zeyu[1], HUANG Fuxiang[1,2] (1. Tianjin University, School of Materials Science and Engineering, Tianjin, 300072, China; 2. Pipeline Research Institute of CNPC, Langfang, 065001 Hebei, China). p 77—80

Abstract: The pipeline internal circumferential automatic welding machine (PIW machine) has been mainly used for pipe alignment and welding root pass in course of pipeline construction. Compared with the other root pass equipment and technologies, PIW machine has the higher efficiency and better root quality. This paper researches the key technologies such as the entire design of PIW machine with multi-torches, digital control system, arc-control for small size wire and the internal welding process. The site application indicates PIW machine with multi-torches has the advantages of reasonable structure and advanced control system, its welding speed is 90s per joint. Its reliability and the filed adaptability to environment meet the site welding construction request completely.

Key words: pipeline; internal circumferential joint; multi-torch; automatic welding machine; root pass

Microstructure transformation and mechanical properties of TC4 alloy joints welded by TIG WU Wei, CHENG Guangfu, GAO Hongming, WU Lin (State Key Laboratory of Advanced Welding Production Technology, Harbin Institute of Technology, Harbin 150001, China). p 81—84

Abstract: The microstructure and phase transformation of TC4 alloy weld joints during TIG welding were investigated. The mechanical properties of the welded joints were also tested. When the TC4 alloy was heated by TIG arc, grains in the weld bead and heat affected zone (HAZ) were badly coarsening. The grain size in HAZ has mutant character. The microstructure in the transition region presented zonal distribution. There was no obvious fine grained region. In temperature-rise period, the transformation of $(\alpha+\beta)\rightarrow\beta$ was divided into two processes which included the original $\beta\rightarrow$ high-temperature β and the original $\alpha\rightarrow$ high-temperature β. And the previous phase transformation was finished before the next starting. In the cooling process, slowly cooling rate introduced α' phases nucleating at the high-temperature β grain boundary in the $\beta\rightarrow\alpha$ transform temperature range. The α' martensite grew up into the center of the β grains and generated acicular martensite. With quicker cooling rate, large numbers of α' phase nucleated in the high-temperature β grains and generated orthogonally oriented martensites. Hardness measurements show there is a softened zone in HAZ. Tensile strength of welded joint was approximate with the base metal. And the properties of the welded joints were good.

Key words: TC4; heat-affected zone; microstructure transformation; mechanical properties

Content of nitrogen and property of deposited metal of self-shielded fluxed-cored wires WANG Qingbao[1,2], SHI Lipeng[1,2], WANG Lizhi[1,2] (1. MCC Welding Science & Technology Co, lid, Beijing 100088, China; 2. Welding Research Institute, CRI BC, MCC, Beijing 100088, China). p 85—88

Abstract: Using the self-shielded fluxed-cored wires of deposited metal with 00Cr13Ni4Mo, the number of layer, the welding temperature, welding velocity, current and voltage are, the other welding parameters are hold the line. The different changing solely content of nitrogen, the metallographic structure and hardness were studied. The results show that the welding parameters have greatly effect on the content of nitrogen, the metallographic structure and hardness. In repairing the continute rollers, welding parameters must be carefully considered especially for the open arc welding process.

Key words: welding parameter; number of welding layer; welding temperature; welding velocity

Application of substructure and submodelling on 3D numerical simulation of welding ZENG Zhi[1], WANG Lijun[1], ZHANG Han[2] (1. School of Materials Science and Engineering, Tianjin University, Tianjin 300072, China; 2. Julong Steel Pipe Co., Ltd. Qingxian 062658, Hebei, China). p 89—93

Abstract: For the computing time and accuracy in the numerical simulation on welding residual stresses and distortion of large structure, an effective finite element method with substructure and submodelling was developed in this paper. The theory models of substructure and submodelling were represented, both applied condition